Forest structure and its changes from multi-temporal lidar data: a homogeneously derived database for peninsular Spain

Mihai A. Tanase[1,2]✉, Juan Pablo Martini[1], Daniel Garcia Garcia[1], Miguel Á. Zavala[3], Paloma Ruiz-Benito[1,3]

Abstract Monitoring Forest structure across large and heterogeneous landscapes is essential to understanding ecosystem dynamics, carbon stocks, and the impacts of global change. This study leverages lidar surveys from Spain's national airborne laser scanning (ALS) program to produce harmonized, high-resolution maps of canopy height, canopy cover, and aboveground biomass (AGB) across peninsular Spain over two periods: 2008-2016 and 2015-2021. We developed a consistent processing workflow to overcome challenges posed by heterogeneous lidar acquisitions, and integrate the resulting metrics with National Forest Inventory (NFI) data to model AGB using machine learning algorithms. Validation against field data demonstrated high accuracy for canopy height ($R^2 > 0.8$; RMSE < 3 m in some regions) and acceptable performance for AGB estimation (RMSE: 23–44 t ha^{-1}). Between the two lidar surveys, forests exhibited structural development in forest canopies, with average annual increases of 0.2 m in height and 0.9% in canopy cover, particularly pronounced in the Atlantic regions. Species-level analysis highlighted the structural and functional contrast between biomes: high-biomass Atlantic species such as *Fagus sylvatica* and *Pinus radiata* reached up to 188 t ha^{-1} and 126 t ha^{-1} AGB, respectively, while Mediterranean species like *Quercus ilex* and *P. halepensis* remained under 35 t ha^{-1}. Comparisons with global and regional satellite-derived products revealed that airborne lidar offers superior spatial detail and accuracy, especially in structurally complex forests. ALS-based height estimates showed significantly lower mean absolute error (MAE: 1.6–3.7 m) than global products (MAE: 2.9–7.8 m), while GEDI data consistently overestimated canopy height, 5.9 m on average, across the peninsular Spain. This work highlights the critical role of harmonized lidar datasets for robust forest monitoring, and provides a valuable baseline for future ecological assessments, carbon accounting, and validation of satellite products across the peninsular Spain.

Addresses: [1]Department Geología, Geografía y Medio Ambiente, Grupo de Investigación en Teledetección Ambiental, Universidad de Alcalá, Alcalá de Henares, Spain. | [2]Instituto de Ciencias Forestales ICIFOR (INIA-CSIC), Madrid, Spain. | [3]Departamento de Ciencias de la Vida, Grupo de Ecología y Restauración Forestal (FORECO), Universidad de Alcalá, Alcalá de Henares, Madrid, Spain.

✉ **Corresponding Author:** Mihai A. Tanase (mihai.tanase@tma.ro).

Introduction

Forests play a critical role in environmental, social, and economic domains by providing essential ecosystem services such as climate regulation, soil stabilization, water purification, habitat provision, and recreational opportunities (Bonan 2016, Pan *et al.* 2018).

Globally, forests represent key terrestrial ecosystems, storing approximately 45% of terrestrial carbon and significantly mitigating anthropogenic CO_2 emissions through their role as carbon sinks or sources, depending on disturbances and management practices (Houghton *et al.* 2015, Buotte *et al.* 2020). However, since the last century, these vital ecosystems have been facing increasing threats from anthropogenic and environmental disturbances, leading to habitat degradation and a diminished provision of ecosystem services (Senf *et al.* 2017, Senf & Seidl 2020).

As disturbances have intensified globally, approximately 77 million hectares of forests are lost annually to wildfires and biotic disturbances (Senf & Seidl 2020). In Europe alone, disturbances impacted around 17% of forests over the past two decades. In particular, Spain experienced increasingly severe wildfire seasons, with 2022 and 2025 being some of the worst in the past decade, highlighting the vulnerability of Mediterranean forest ecosystems to disturbance events (San-Miguel-Ayanz 2023). Therefore, reliable and consistent monitoring of forest structure (e.g. canopy height and cover, and aboveground biomass) is crucial for understanding forest dynamics, carbon emissions, and informing effective forest management strategies in the face of unprecedented global changes (Lang *et al.* 2023).

Traditional forest monitoring methods, typically field-based such as National Forest Inventories (NFIs), provide accurate local data but are limited by their spatial coverage, frequency, and high operational costs (Tomppo *et al.* 2010, Hudak *et al.* 2020). Consequently, NFIs often fall short in delivering timely, large-scale, and synoptic information critical for forest management and policies development. Such limitations have been partially addressed using remote sensing technologies, to significantly overcome the spatial-temporal constraints associated with field-based inventories (Wulder *et al.* 2020).

Remote sensing technologies, including optical, radar, and particularly lidar (from light detection and ranging), offer robust methodologies for capturing forest structural information at various scales (Fassnacht *et al.* 2016, White *et al.* 2016). Lidar technology stands out as the most precise remote sensing method for estimating forest structural attributes due to its ability to provide three-dimensional representations of canopy structure, height, and cover (Dubayah *et al.* 2020, Potapov *et al.* 2021).

Lidar measurements significantly improve accuracy compared to optical or radar methods, and have become critical in calibrating and validating other remote sensing datasets, despite limitations in cost and temporal availability (Matasci *et al.* 2018, Hudak *et al.* 2020, Tanase *et al.* 2026).

Recent studies have demonstrated the value of multi-temporal airborne lidar datasets for assessing temporal changes in forest structure. For example, bi-temporal airborne lidar was combined with Landsat imagery to quantify structural changes following wildfire in western U.S. forests, with strong correlations being found between the lidar-derived canopy height changes and field-measured burn severity (McCarley *et al.* 2017).

Forest structure changes were quantified with temporal lidar data within direct and indirect detection strategies (Mauro *et al.* 2019) while canopy and surface fuel loads were estimated before and after fires (Bright *et al.* 2022). Such studies underscore that multi-temporal lidar may become a robust tool for monitoring forest structural dynamics, enabling quantification of disturbance impacts and recovery over time.

In response to growing environmental and management demands, many European countries (e.g., Spain, Finland, Sweden,

Austria, France, Germany) have developed national lidar programs providing systematic airborne lidar coverage at national scales. Such initiatives are essential to obtain detailed forest structural information across spatial and temporal scales. However, integrating data from multiple lidar flights introduces challenges due to variations in sensor characteristics, flight parameters, and point density across temporal acquisitions. These variations can lead to inconsistencies, complicating forest change monitoring over large areas. Indeed, despite its national scope and open availability, the Spanish PNOA-Lidar program (from the Spanish "Plan Nacional de Observación Aérea") presents notable challenges for multi-temporal forest monitoring due to its decentralized implementation. Data are acquired regionally over extended periods, often years apart, resulting in temporal mismatches that complicate consistent change detection across the country. Additionally, acquisitions are performed by different contractors using various lidar sensors and flight configurations, leading to inconsistencies in point density, scan angles, and positional accuracy. These differences may propagate into the derived products such as digital elevation models (DEMs) and canopy height models (CHMs), affecting the comparability of structural forest attributes like tree height or aboveground biomass (AGB) over time. Therefore, to ensure robust temporal analysis, it is essential to implement workflows that correct for acquisition-specific biases. For example, the use of a common DEM for height normalization ensures temporal consistency of forest structural attributes, thereby enabling more reliable detection and quantification of changes in forest height estimates (Coops *et al.* 2021).

This study aimed to leverage the first two PNOA-Lidar national surveys to generate homogeneous forest structural information across peninsular Spain. Specifically, our objectives were to i) derive spatially and temporally consistent estimates of forest canopy height, canopy cover, and AGB from multi-temporal lidar data; ii) analyze changes in forest structure at regional to national scale;

and iii) compare our estimates with global and continental remote sensing products available for the Iberian Peninsula. As such, this study contributes to improving forest monitoring and management strategies, informing policies, and enhancing our understanding of the dynamic changes occurring in peninsular Spanish forests due to climatic and anthropogenic influences.

Material and methods

Study area

The research was focused on the peninsular Spain, southwestern Europe, and includes 15 autonomous regions (henceforth regions). Covering approximately 493,000 square kilometers, the area stretches from the Atlantic coast in the northwest to the Mediterranean shores in the southeast. The territory is characterized by a markedly varied topography that includes broad coastal plains, rolling hills, and prominent mountain systems such as the Pyrenees in the northeast and the Sierra Nevada in the south, where elevations can exceed 3,400 m a.s.l. Such physical heterogeneity gives rise to a wide array of climatic and ecological zones, and therefore, forest ecosystems (Blanco Castro *et al.* 2005).

The Mediterranean climate dominates much of the peninsula and is characterized by prolonged dry summers and wetter mild winters. In contrast, the northern coastal areas experience an oceanic (Atlantic) climate, marked by consistent precipitation throughout the year and cooler summer temperatures. Some interior and southeastern regions exhibit semi-arid conditions, with low annual rainfall. Precipitation varies across the country, ranging from under 300 mm per year in the southeastern provinces to more than 2,000 mm in the Atlantic region. Likewise, thermal regimes are diverse, with average monthly temperatures below freezing in winter at high altitudes and above 35 °C during the summer in southern inland Spain.

Vegetation cover reflects the environmental diversity. Approximately 50% of the land

surface is occupied by forests and shrub-dominated landscapes (EUROSTAT 2022). Forest composition and structure variation is largely driven by climatic gradients. In the drier, fire-prone Mediterranean biome, sclerophyllous evergreen species such as *Quercus ilex* (holm oak) and *Q. suber* (cork oak) dominate, being frequently accompanied by drought-tolerant pine species including *Pinus halepensis*, *P. pinea*, and *P. pinaster*. In the temperate Atlantic regions, the forest composition shifts towards deciduous broadleaf species, notably *Fagus sylvatica* (European beech) and a range of oak species (*Q. robur, Q. petraea, Q. pyrenaica*), alongside plantations of non-native species such as *Pinus radiata* and *Eucalyptus* species. Mixed stands combining deciduous and evergreen species are also common, especially in transitional zones. The resulting landscape is a mosaic of forest types, influenced not only by natural ecological gradients but also by centuries of land use, including agriculture, grazing, forestry, and abandonment (Blondel & Aronson 1995). Forest structure exhibits substantial heterogeneity. In mountainous and humid areas, forest stands tend to be taller and denser, while in Mediterranean lowlands, the vegetation is sparser and includes shrublands and low forest canopy heights (Lines *et al.* 2012). Such structural and compositional complexity poses significant challenges for ecological monitoring and forest management across the peninsula.

Lidar data

The lidar data were downloaded, in compressed format (LAZ), from the Spanish National Center for Geographic Information (CNIG) as classified point clouds. The PNOA-Lidar project, aims to generate periodic (every five years) three-dimensional information across the national territory using airborne lidar sensors (Table 1). However, in practice, the time span between flights is often higher (Figure 1).
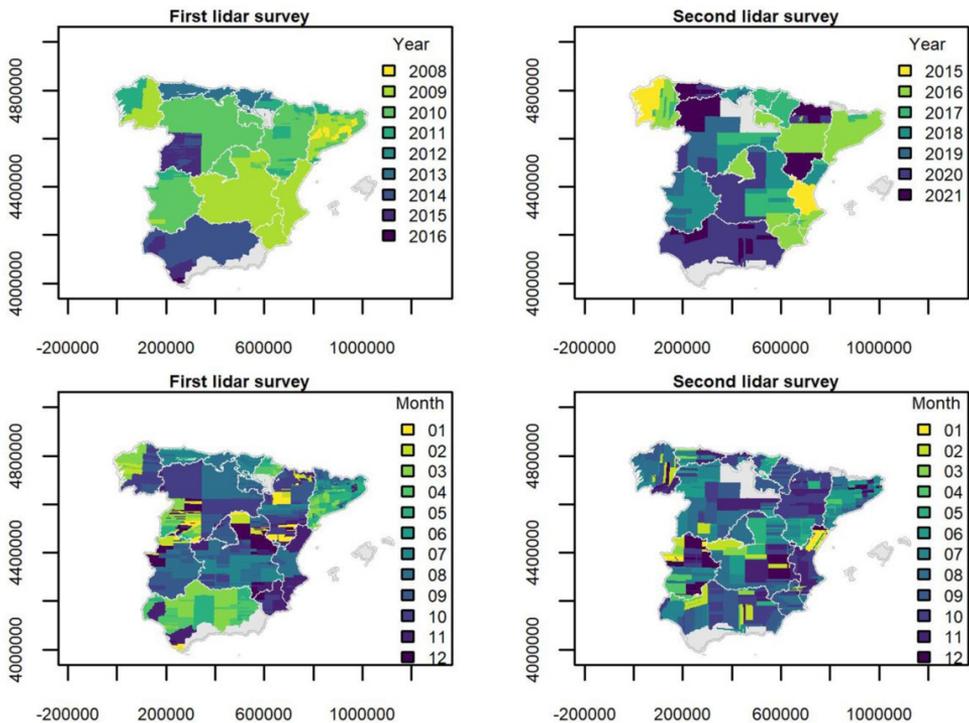
Figure 1 Acquisition years and months for the first and second national lidar surveys across peninsular Spain. Flight lines with missing date or time information are shown in grey. Seasonal variability in acquisition conditions (i.e., month of capture) is evident both between and within regional surveys.

Table 1 Main characteristics of the lidar flights acquired under the PNOA-Lidar project.

Flight	Flight year	Point density per m²	Target error		Grid size (km)
			xy (m)	z (m)	
First	2009 - 2016	0,5	0,3	0,2 - 0,4	2x2
Second	2015 - 2021	0,5 - 4 *	0,2 - 0,3	0,15 - 0,2	2x2

* Point density for Navarra second flight was 14 point /m².

Point clouds were processed at regional level to extract the forest attributes (i.e. height, canopy cover) as well as the lidar metrics used for above ground biomass modelling (e.g., height percentiles, returns proportion in five-meter strata, first return counts.

Data processing followed a largely standardized workflow (Figure 2), using primarily the LAStools software (van Rees 2013). Slight variations in the workflow occurred depending on the regional flight's characteristics. Workflow deviation (i.e., refinement), for each flight and region, was the result of a preliminary analysis conducted in three to ten test zones depending on region size. Each test zone consisted of nine tiles covering 36 km². The preliminary analysis resulted in a per region customized processing chain which was applied to the bulk data to generate the forest variables and lidar metrics of interest. The analysis included the generation of a 10-meter resolution DEM using the points classified as ground over the test tiles. Visual inspection was conducted to identify classification errors, especially in dense vegetation areas (see example in Figure 3).

Detected errors, typically due to vegetation points misclassified as ground, were corrected by reclassifying ground points with the `lasground_new` tool or the MCC-LIDAR tool (Evans & Hudak 2007) depending on the reclassification success. Reclassification parameters were determined through an iterative analysis (Supplementary Table S1).

Other common issues were related to increased point densities for specific vegetation classes as well as tiles available with different coordinate reference systems within the same region.
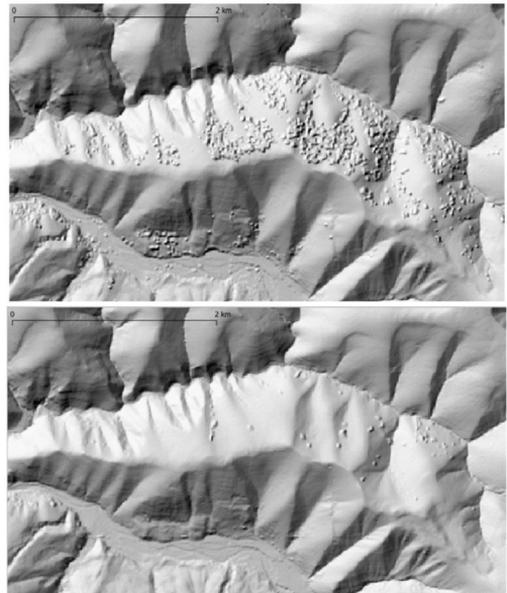
Figure 3 Subset of the shaded digital elevation model before (left panel) and after (right panel) reclassifying the ground class using *lasground_new* tool. Data from the second lidar survey (2018) in Cantabria.
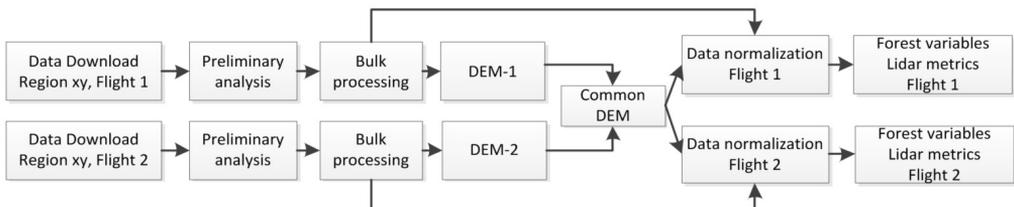
Figure 2 Lidar data processing workflow used to produce Digital Elevation Models (DEMs) and compute forest structural variables. A preliminary analysis on representative test areas was used to optimize the processing chain for each regional survey. Bulk processing corresponds to the application of the finalized chain to all regional lidar tiles. Data normalization adjusts raw elevation values relative to the ground surface (height above ground).

The bulk data processing chain included retiling both lidar surveys to a common grid for subsequent height normalization. After bulk data processing the resulting raster layers were inspected and the chain was further adjusted when needed.

To enhance consistency across flights and facilitate temporal analysis, a combined DEM was generated using the 50th percentile height of points classified as ground from the first two lidar flights, assuming constant topography. During processing, special attention was given to the provided vegetation classification to identify and correct anomalies typically encountered for specific flight lines.

Forest attributes and lidar metrics were computed at a 10-meter resolution for each tile and flight. Lidar metrics included height percentiles (p05, p15, p30, p50, p75, p98, in meters), point densities above 2 m (i.e., the tree stratum), by height stratum (e.g. 2–5, 2–10, 5–10, 10-15, 10-20 m), return counts (ground, first, and all returns), and canopy cover fraction (FCC, %), calculated as the ratio of first returns above 2 m to all first returns. Additional metrics included height skewness (SKE), height standard deviation (STD), vertical complexity index (VCI) describing the vertical structural diversity of vegetation (van Ewijk *et al.* 2011), quadratic mean height above 2 m (QAV), kurtosis (KUR), and height of median energy return (HOM).

For each lidar survey, the tile-level lidar metrics were mosaicked to produce wall-to-wall maps at the regional scale, supporting spatial analysis and inter-flight comparisons.

Forest National Inventory data

To assess the precision of lidar-derived forest attributes (height and canopy cover) and to estimate aboveground biomass (AGB) across peninsular Spain, we used data from the Spanish National Forest Inventory (NFI; Table 2). The Spanish NFI is compiled and published by the Ministry for the Ecological Transition and the Demographic Challenge (MITECO) and provides nationally consistent information on forest structure, composition, and biomass across Spain that may be used to calibrate and validate remote sensing products as the geographic location is also collected (Villaescusa & Díaz 1998).

The NFI sampling design is based on a regular 1 × 1 km grid, with a single permanent plot (25 m radius) being established at each grid intersection when falling within forested areas (Sanz & Soto 1990). Within each sample plot, tree-level measurements are recorded using a variable-radius design for trees above 130 cm

Table 2 Regional mean values and standard deviation (in parenthesis) for forest structural variables according to the 4th Spanish National Forest Inventory (NFI). NFI data for Andalusia and Valencia were not available.

Region	Field data collection	No. of plots	Mean values and standard deviation (in parenthesis)		
			Tree height (p98th, m)	Forest canopy cover (%)	Above-ground biomass (t ha-1)
Aragon	2021-2022	4,502	12.4 (5.5)	61.5 (19.5)	72.4 (66.9)
Asturias	2009-2010	2,304	19.9 (6.5)	65.4 (22.5)	124.2 (97.2)
Basque Ctr.	20101	1,622	21.7 (8.7)	77.4 (16.5)	139.7 (94.7)
Castile la Mancha	2020-20212	6,924	11.7 (5.2)	53.0 (20.3)	50.7 (45.7)
Castile and Leon	2018-2019	10,143	13.9 (6.5)	61.5 (20.8)	81.2 (70.6)
Cantabria	2009-2010	1,647	19.4 (7.7)	68.7 (21.6)	131.2 (100.6)
Catalonia	2014-2016	4,489	15.0 (5.9)	71.2 (17.2)	90.6 (67.8)
Extremadura	2016-2017	2,560	11.3 (4.9)	51.4 (21.8)	48.8 (44.2)
Galicia	2008-2009	7,612	21.8 (8.7)	62.8 (21.7)	106.2 (84.9)
La Rioja	2011-2012	1,229	15.9 (6.9)	70.7 (18.8)	119.3 (85.6)
Madrid	2012-2013	1,206	12.2 (5.4)	54.8 (21.2)	72.6 (65.3)
Murcia	2010	1,284	9.9 (2.9)	50.5 (18.4)	28.7 (21.1)
Navarra	2008	2,943	19.0 (8.2)	73.5 (20.3)	142.3 (99.3)

[1] 34 plots collected in 2011; [2] 373 plots collected in 2019.

in height. Tree selection radii varies: trees with DBH between 7.5 and 12.4 cm are sampled within a 5-meter radius; those between 12.5 and 22.4 cm within a 10-meter radius; trees between 22.5 and 42.4 cm within a 15-meter radius; and trees with DBH exceeding 42.4 cm within a 25-meter radius. Tree height is measured using hypsometers while canopy cover is visually estimated.

Aboveground biomass at tree level was calculated using species-specific allometric equations (Montero *et al.* 2005), which relate DBH to biomass (eq. 1 to 3). When species-level identification was not available, biomass was estimated at the genus level (Ruiz-Benito *et al.* 2014).

Plot-level AGB (in t ha⁻¹) was then derived by summing tree-level estimates and applying linear scaling factors based on the plot's sampling design (Henttonen & Kangas 2015). Where the acquisition dates of Lidar and NFI data did not coincide (Figure 1 and Table 2), we accounted for temporal discrepancies by estimating forest productivity (t ha⁻¹ yr⁻¹) from permanent plots measured in both the third and fourth NFI cycles (Ruiz-Benito *et al.* 2014).

For each region, productivity rates were calculated and averaged by forest species. These rates were used to adjust the AGB values reported in the fourth NFI to correspond with the year of the Lidar acquisition used to derived the cartographic products (eq. 4).

$$AGB = CF * A * d^b \qquad (1)$$

$$CF = e^{\frac{SEE^2}{2}} \qquad (2)$$

$$A = e^a \qquad (3)$$

where: AGB – above-ground biomass, CF – correction factor, SEE – standard estimation error, d – diameter at breast height, a and b – species specific coefficients. Coefficients (a, b) and SEE as per Table 2 in Moreno et al. (2025).

$$AGB\_adjusted = AGB\_NFI \pm (Productivity \times \Delta Years) \qquad (4)$$

where: AGB – above-ground biomass, NFI – national forest inventory.

Above-ground biomass modelling

To generate wall-to-wall AGB cartographic products, we integrated lidar-derived metrics with auxiliary topographic variables (i.e., elevation, slope, aspect, and surface roughness) and categorical information on dominant forest species. For each NFI plot, we extracted lidar and topographic data using a 25-meter radius buffer centered on the plot location. Forest species composition at each plot was identified using the latest regional forest map (Bombín 2005) which allowed for the inclusion of main species ID as a predictor variable. Notice that due to the lack of *in-situ* NFI data (Table 2), AGB maps for Andalusia and Valencia region were not computed.

Two types of machine learning (ML) algorithms were evaluated independently in each region: Random Forests (Breiman 2001) and Extreme Gradient Boosting (Friedman 2001).

The Random Forests (RF) algorithm constructs an ensemble of regression trees using bootstrapped samples of the training data (with replacement) and aggregates predictions to minimize overfitting.

In contrast, Extreme Gradient Boosting (XGB) builds predictive models in a sequential manner, iteratively combining multiple weak learners (typically shallow decision trees), each with limited individual predictive power but capable of improving overall model performance when combined (Freund & Schapire 1997).

To mitigate overfitting and reduce redundancy among predictor variables, we screened the lidar-derived metrics to exclude the highly correlated ones (Pearson's |r| > 0.7). Among each group of correlated variables, only the metric with the highest correlation with AGB was retained. From this filtered set, the top 13 metrics, ranked by variable importance within an initialization run for RF model, were selected for inclusion in the final AGB modeling framework.

The data was randomly partitioned into training (90%) and validation (10%) subsets

across 15 independent iterations. For each iteration, AGB models were trained and applied to generate spatial predictions. The final AGB map was constructed by averaging the outputs of the 15 individual models while model uncertainty at the pixel level (standard error) was computed using the predicted value of all model runs.

Model performance was evaluated for each run using standard metrics, including mean error (ME, eq.5), mean absolute error (MAE, eq. 6), root mean squared error (RMSE, eq. 7), relative RMSE (rRMSE, eq. 8) and the coefficient of determination (R²) between observed and predicted AGB values. Model performance was reported as the mean value across the 15 runs.

The final AGB map was selected based on the comparative performance of the RF and XGB models. For approximately half of the regions (i.e., Aragon, Basque Country, Castile la Mancha, Catalonia, Galicia, and Madrid) the RF model demonstrated superior predictive accuracy (higher R^2 and lower RMSE) and was adopted. For the remaining regions, the XGB-based AGB maps were retained due to their comparatively better performance.

$$ME = \frac{1}{n} \sum_{i=1}^{n} \hat{y}_i - y_i \qquad (5)$$

$$MAE = \frac{1}{n} \sum_{i=1}^{n} |\hat{y}_i - y_i| \qquad (6)$$

$$RMSE = \sqrt{\sum_{i=1}^{n} \frac{1}{n} (\hat{y}_i - y_i)^2} \qquad (7)$$

$$rRMSE = RMSE / \sum_{i=1}^{n} \frac{1}{n} (y_i) \qquad (8)$$

where $\hat{y}_i$ and y_i represent predicted and observed AGB values, respectively, and n is the number of validation observations.

Lidar products validation and analysis

We quantified the agreement between key structural lidar-derived metrics (i.e. 98th height percentiles, p98 and the canopy cover fraction, FCC) and *in-situ* NFI estimates to provide insights into the accuracy and robustness of

PNOA-Lidar data for characterizing forest vertical structure and canopy density across diverse biogeographic contexts (for AGB product validation see relevant section above). The evaluation was carried out by region, and considered the time lag between *in-situ* NFI collection date and the lidar survey date for each individual flight line.

To highlight general structural features and identify temporal trends in forest canopy development and stratification we performed a descriptive analysis of the spatial distribution of median values using the lidar-derived forest attributes across peninsular Spain. This provided a broad-scale perspective of forest changes between the two lidar flights, as well as a means to validate global cartographic products derived from satellite data. To understand forest structural distribution across ecologically contrasting landscapes regional analyses were carried out after stratifying by the dominant forest species. For each region only species representing at least 5% of the territory were individually analyzed.

Cross-comparison with global and regional products

We carried out comparative analyses between the canopy height metrics generated in this study (p. 98) and regional and global vegetation height products (Potapov *et al.* 2021, Lang *et al.* 2023, Tolan *et al.* 2024, Su *et al.* 2025). These studies rely on different sensors and modeling approaches, resulting in a range of spatial resolutions and estimation periods (Table 3). Potapov et al. (2021) used machine learning to extrapolate GEDI footprint heights with Landsat time-series data to produce a global canopy height map. Lang et al. (2023) generated a global canopy height model using a deep-learning ensemble that combines Sentinel-2 imagery with GEDI RH98 metric. Tolan et al. (2024) developed a canopy height product from Maxar RGB imagery using a self-supervised vision tranŷsformer trained on aerial lidar canopy-height models and refined

Table 3 Global and regional products of forest attributes over the peninsular Spain.

Database	Predictor / Reference	Modelling	Product year(s)	Resolution	RMSE
Potapov et al. (2021)	Landsat / GEDI	Machine learning	2019	30 m	6 – 9 m
Lang et al. (2022)	Sentinel-2 / GEDI	Deep learning	2020	10 m	6 m
Tolan et al. (2024)	MAXAR GSD / GEDI	Deep learning	circa 2018-2020	1 m	1.8 - 3 m
Su et al. (2025)	Sentinel-1 & Sentinel-2 / ALS, GEDI	Deep learning	2017 to 2021, yearly	10 m	2- 3 m 29 Mg ha^{-1}

with a GEDI-based calibration network.

Lastly, Su et al. (2025) produced regional annual maps of canopy height and aboveground biomass for the Iberian Peninsula using U-Net models integrating Sentinel-1/2 imagery with ALS and GEDI data. The analysis focused on regions with ALS PNOA surveys available within one year of the satellite data used to generate the regional or global products: i.e., Andalusia, Aragon, Castile la Mancha, Castile and Leon, Extremadura, Asturias, Cantabria. These regions represent all climatic gradients and biomes in the Iberian Peninsula. In each region, we selected only the relevant ALS flight lines as PNOA surveys may span several years (Figure 1). It should be noted that a preliminary analysis comparing ALS and satellite-derived products using only contemporaneous data (same year) showed negligible differences. To evaluate the agreement between the lidar and satellite derived height we used R², ME, MAE, RMSE, and rRMSE. As Su et al. (2025) provide annual products (2017 to 2021) for both canopy height and biomass, we used the corresponding NFI data to evaluate the accuracy of their products.

As comparison of GEDI derived heights (rh98) with *in-situ* NFI data was not feasible due to the spatial mismatch between both datasets, the PNOA ALS height (P98) was used to benchmark this widely used product. To ensure similar vegetation phenology, only GEDI footprints acquired within the same season as the lidar survey were used. For Andalusia, Aragon and Asturias the comparison with GEDI footprints was carried out in 2020 and 2021, for Cantabria and Extremadura in 2022, for Castile la Mancha in 2019 and 2020, and for Castile and Leon in 2019, 2020 and 2021. In the Madrid region the GEDI footprints acquired in 2022 and 2023 were compared with the third lidar survey from 2024 as, in the absence of natural disturbances, vegetation changes are negligible as per the FNI growth rates.

Results

Validation of lidar-derived forest attributes

The accuracy of lidar-derived estimates of forest height and canopy cover varied among regions and, within each region, depending on the time lag between the *in-situ* data collection and the lidar survey (Table S2). Across regions, the ALS derived forest height was within 0.2 m (mean error) when assessed against *in-situ* plots collected within one year of the lidar survey. Forest cover estimates were 25% higher with respect to the visual *in-situ* assessments. It should be noted that Galicia was not included when calculating mean values across the peninsula as about 50% of the region was acquired during leaf-off conditions in the first lidar survey, the temporally closest with FNI data collection.

For tree height, the highest R² (> 0.8) and lowest rRMSE (<15%) values were observed for forest located in Castile la Mancha, Castile and Leon, La Rioja and Navarra. For most of the remaining regions and flights the rRMSE was below 25% and R² above 0.65. Higher rRMSE values (~40%) coupled with lower R² values (<0.4) were observed for forest height in Cantabria and Galicia when ALS data was acquired more than one year after the *in-situ* measurements. The smallest R² (0.04) and largest rRMSE values (173%) were observed

11

in Catalonia for NFI plots collected in 2015. Across regions, the rRMSE was 18-19%, when assessed against NFI plots collected within one year of the lidar survey. The effect of the temporal lag between *in-situ* data collection and the lidar survey was not consistent across regions. In the northern Atlantic forests, the accuracy of ALS estimates declined markedly with increasing lag - for instance, in Cantabria, the rRMSE doubled from 19% to 38%. In contrast, this effect was less pronounced in the Mediterranean forests: in Castile-La Mancha, model precision remained nearly unchanged regardless of the lag, while in Aragon, Extremadura, and La Rioja, the rRMSE increased by only 3–5% when the lag exceeded one year.

The disagreement between FCC lidar estimates and the *in-situ* NFI data was large, with rRMSE reaching about 35% in the Atlantic forests and 50% in the Mediterranean ones for temporal lags of one year or less. For higher temporal lags the difference to NFI estimates increased by 12% and 5% respectively. Furthermore, it seems that increasing differences were sometimes related to particular flight lines. Such inconsistencies were observed for Catalonia and to a lesser extent for Extremadura where differences were higher for a time lag of two years when compared to a time lag of three years.

The largest relative error when estimating AGB occurred in Aragon (rRMSE = 69.8 %), when excluding western Galicia where the lag between the NFI campaign and the lidar acquisition exceeded five years (Table S4). The lowest rRMSE (39.8 %) was observed in the Basque Country. Across the peninsula, AGB estimation error was 58.5%.

Forest structure dynamics

Between the first and the second lidar survey, the canopy height (P98) increased at an annual rate of 0.2 m while the forest canopy cover (FCC) increased at an annual rate of 0.9%, except for FCC in Asturias, Catalonia, La Rioja and Murcia where FCC change was -0.1% y^{-1}

(Figure 4 and Table S3).

These average values disregard changes in Galicia (0.8 m y^{-1} and 5.7% y^{-1}) which were partially influenced by the leaves off conditions and the presence of deciduous species, for about half of the region, at the time of the first lidar survey. By biome, excluding Galicia, higher annual increase rates (0.33 m y^{-1}) were observed in the Atlantic forests (Asturias, Cantabria, Basque Country, Navarra) when compared to the Mediterranean forests (0.12 m y^{-1}). The mean AGB values and standard deviation (SD) across peninsular Spain, excluding Andalucía and Valencia regions where no data were available, is 77.5 (35.3 SD) t ha^{-1}, ranging from 139.2 (74.8 SD) t ha^{-1} in the Basque country to 20.4 (15.2 SD) t ha^{-1} in Murcia (Table S4).

Canopy structure metrics highlight biome-level differences for the dominant forest species (Figure 5 and Table 4).

In the Atlantic biome, coniferous species such as *Pinus radiata, P. sylvestris* and P. *pinaster* exhibit high canopy cover (FCC > 55%) and heights (13–16 m), reflecting humid temperate conditions. Similarly, broadleaved species such as *Fagus sylvatica* and *Quercus robur* reach significant heights (14–18 m) and canopy cover (70-75%) values in the north. In contrast, across the Mediterranean biome, more conservative values were observed: for species common to both biomes, the average forest height was 15% to 50% lower across the Mediterranean when compared to the values observed in the Atlantic regions.

FCC followed a similar trend but only for the deciduous species. In the Mediterranean, the dominant pines like *P. halepensis, P. nigra*, and *P. sylvestris* reach moderate canopy cover (FCC 45–60%) and reduced heights (10–12 m), as growth limitations are imposed by summer droughts and poorer soils. Evergreen oaks such as *Q. ilex* display moderately dense, canopies and shorter tree (~45% FCC, <10 m tall), consistent with sclerophyllous adaptations to water scarcity. By species, the highest mean AGB was observed for *F. sylvatica* (188.0 ± 0.09 t ha^{-1}) followed by
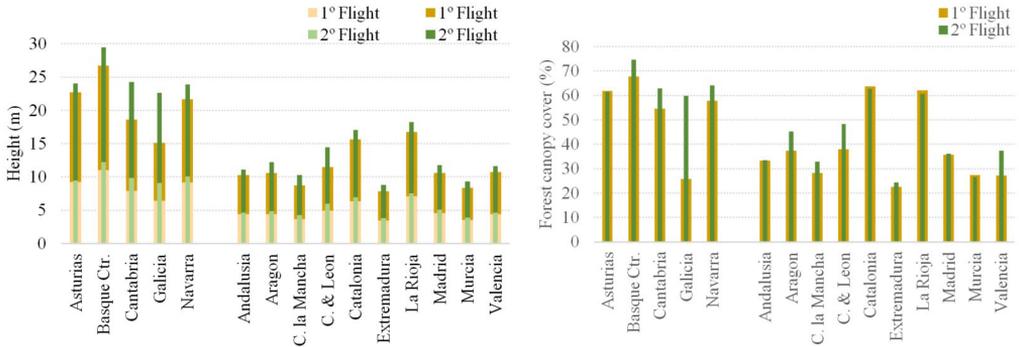
Figure 4 Average forest height and canopy cover by region for the first and second national lidar surveys. Regions in the Atlantic biomes are shown to the left of the gap, regions in the Mediterranean biomes are shown to the right of the gap.
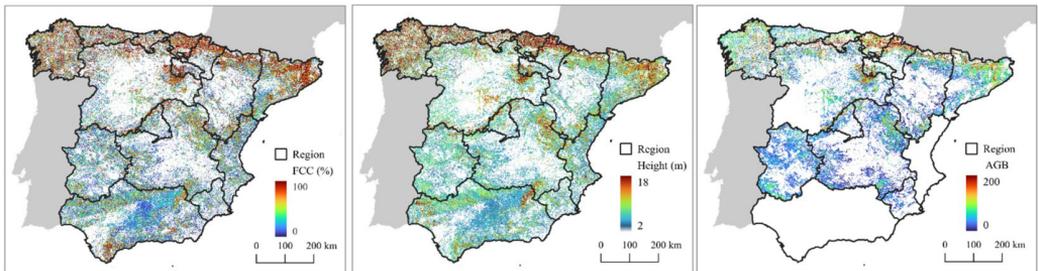
Figure 5 Spatial patterns of forest canopy cover (FCC), height (98th percentile), and above ground biomass (AGB) across peninsular Spain. AGB derived for the lidar survey temporally closest to the in-situ data collection. FCC and P98 derived from the second lidar survey.

Table 4 Mean forest height, canopy cover (FCC), and aboveground biomass (AGB) by biome and species. Only species covering ≥5% of forest area in at least one region (per the Spanish forest map) were included. Mean values and standard error (± SE) are pooled by biome. Height and FCC are from the second lidar survey; AGB corresponds to the lidar date closest to NFI measurements. Data from Galicia were excluded.

Atlantic forests				Mediterranean forests			
Species	**Height (m)**	**FCC (%)**	**AGB (t/ha)**	**Species**	**Height (m)**	**FCC (%)**	**AGB (t/ha)**
P. sylvestris	13.4 ± 0.002	68.1 ± 0.01	110.3 ± 0.07	*P. sylvestris*	11.5 ± 0.001	67.5 ± 0.01	94.5 ± 0.05
P. halepensis	6.2 ± 0.002	35.4 ± 0.02	45.9 ± 0.06	*P. halepensis*	7.2 ± 0.001	37.6 ± 0.01	31.6 ± 0.02
P. nigra	12.2 ± 0.003	58.0 ± 0.02	98.8 ± 0.09	*P. nigra*	9.4 ± 0.001	53.2 ± 0.01	63.8 ± 0.03
P. pinaster	13.4 ± 0.002	56.6 ± 0.01	70.3 ± 0.03	*P. pinaster*	10.1 ± 0.001	46.2 ± 0.01	65.3 ± 0.04
Q. pyrenaica	11.0 ± 0.002	60.7 ± 0.01	85.1 ± 0.08	*Q. pyrenaica*	8.4 ± 0.001	51.1 ± 0.01	64.3 ± 0.04
Q. faginea	10.0 ± 0.003	70.9 ± 0.02	91.5 ± 0.09	*Q. faginea*	6.5 ± 0.001	46.2 ± 0.01la	37.6 ± 0.04
Q. ilex	7.6 ± 0.003	56.8 ± 0.02	70.1 ± 0.07	*Q. ilex*	4.7 ± 0.001	28.7 ± 0.01	34.4 ± 0.01
F. sylvatica	18.4 ± 0.003	75.9 ± 0.01	188.8 ± 0.09	*F. sylvatica*	17.4 ± 0.004	87.3 ± 0.01	181.1 ± 0.12
Species present in only one biome							
P. radiata	16.4 ± 0.004	58.4 ± 0.01	126 ± 0.09	*P. uncinata*	11.1 ± 0.002	56.0 ± 0.01	145.2 ± 0.07
Q. robur	14.4 ± 0.003	70.2 ± 0.01	110.7 ± 0.08	*P. pinea*	8.0 ± 0.001	39.9 ± 0.01	63.2 ± 0.06
E. globulus	15.4 ± 0.002	56.2 ± 0.01	95.0 ± 0.04	*Q. suber*	6.4 ± 0.001	39.1 ± 0.01	34.7 ± 0.02
C. sativa	15.8 ± 0.002	70.5 ± 0.01	85.4 ± 0.09	*F. angustifolia*	7.8 ± 0.004	40.8 ± 0.03	65.2 ± 0.08
B. alba	18.0 ± 0.004	82.4 ± 0.01	57.6 ± 0.15	*Q. pubescens*	9.3 ± 0.002	60.6 ± 0.01	64.0 ± 0.04
				P.x canadensis	12.7 ± 0.005	36.7 ± 0.02	69.6 ± 0.09

13

P. radiata (126.0 ± 0.09 t ha^{-1}), *Q. robur* (110.7 ± 0.08 t ha^{-1}) and *P. sylvestris* (110.3 ± 0.07 t ha^{-1}). The lowest average AGB were observed for *P. halepensis* (31.6 ± 0.02 t ha^{-1}), *Q. ilex* (34.4 ± 0.01 t ha^{-1}) and *Q. suber* (34.7 ± 0.02 t ha^{-1}).

Lidar-based structural assessment changes between the first and the second lidar surveys reveal distinct trajectories in canopy height and forest cover between Atlantic and Mediterranean biomes (Figure 6). In Atlantic forests, *E. globulus* showed rapid development with mean canopy height increasing from 10.6 m to 15.7 m and forest canopy cover (FCC) rising from 37.6% to 50.6% between the successive lidar surveys. Canopy expansion was also observed for *F. sylvatica*, with FCC increasing from 71.3% to 75.9% and mean height rising by over 1 m. Mediterranean

forests followed more conservative trends. *P. pinaster* and *P. halepensis* experienced modest but consistent gains in both height and FCC, with height increasing by 1.6–1.9 m. *Q. ilex*, a dominant evergreen oak, maintained structurally stable canopies with minor changes. These biome-specific patterns underscore how climate, species traits, and forest management shape structural complexity, with Atlantic stands generally taller and denser than their Mediterranean counterparts.

Comparison with satellite-derived products

When comparing the PNOA ALS tree heights with regional and global products modelled using satellite data as predictor variables (Figure 7 and Table S5), the lowest differences were observed with Su et al. (2025) annual
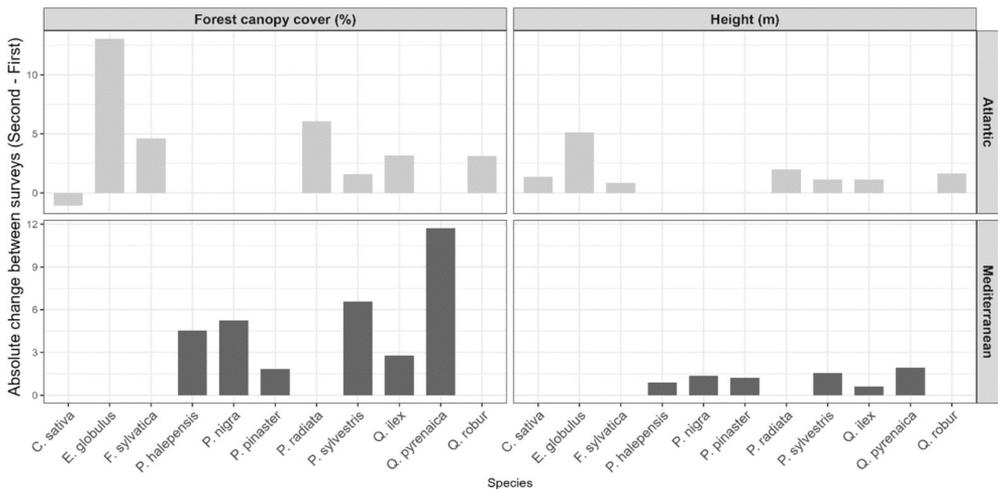
Figure 6 Changes in forest canopy cover (FCC) and forest height between the first and second LiDAR surveys. Bars represent absolute changes by species (mean values across peninsular Spain) in each biome.
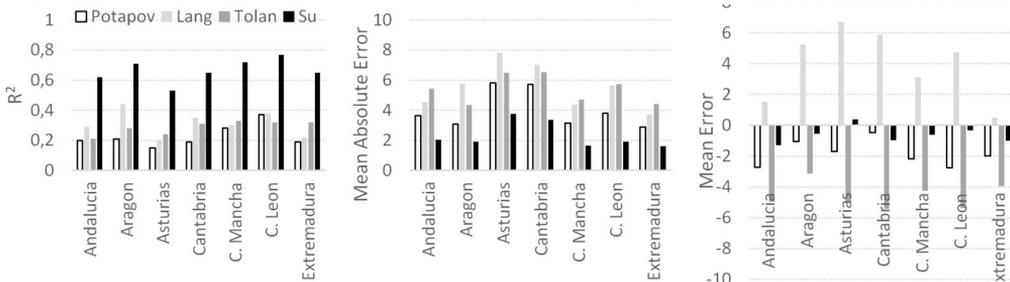
Figure 7 Comparison of forest height (98th percentile) from ALS with regional and global products (Potapov *et al.* 2021, Lang *et al.* 2023, Tolan *et al.* 2024, Su *et al.* 2025). Comparisons use lidar surveys within one year of the satellite product; for Su *et al.* (2025), data are from the same year).

products, with R^2 values ranging between 0.53 and 0.77 depending on the region and MAE between 1.6 and 3.7 m. Except in Asturias, this product underestimated the ALS height by -0.3 to -1.3 m depending on the region.

The height values predicted by global products were considerably different from PNOA ALS estimated height, with the Potapov et al. (2021) providing the closest match (MAE = 2.9-4.0 m), followed by Tolan et al. (2025) with MAE between 4.4-6.5 m and Lang et al. (2023) with MAE values between 3.7 and 7.8 m depending on the region. On average, most products underestimated the ALS height -0.6 m in Su et al. (2025), -1.8 m in Potapov et al. (2021), and -4.6 m in Tolan et al. (2025) while Lang et al. (2023) overestimated the height by 4.0 m.

The largest differences were observed in the Atlantic forests (Asturias, Cantabria) for all products with MAE error increasing by 32% (Tolan), 54% (Lang), 74% (Potapov) and 95% (Su) when compared to the Mediterranean forests.

When assessed against NFI data, the Su et. al. (2025) cartographic products showed larger RSME for height (3.7 to 8.9 m, Table 5) when compared to the ALS product (1.7 to 4.0 m, Table S2).

Similar differences were observed for AGB for the Su et al. (2025) product, with RMSE values increasing by 32% (Castile and Leon) to 120% (Castile la Mancha) when compared to the ALS-derived estimates across the same regions (Table 5 and Table S4).

The comparison of ALS derived height (P98) with GEDI derived height (rh98) showed relatively low R^2 values (0.31 in Castile la Mancha to 0.59 in Aragon) and large RMSE (3.4 m to 9.9 m) as GEDI heights consistently overestimated (+5.9 m) the ALS height (Table 6).

The annual maps developed here can be downloaded, through our interactive web application at https://fodim.uah.es/. To ensure long-term availability, the data have also been deposited in a public repository (see Table S6). All files are provided in GeoTIFF format, ensuring full compatibility with standard GIS software and remote sensing tools.

Discussions

This study demonstrates the feasibility utility and limitations of using multi-temporal airborne lidar data to produce harmonized,

Table 5 Comparison of predicted (Su et al. 2025), and in-situ (NFI) height and above-ground biomass (AGB) by region.

Region	Map year	NFI year	N	R^2	Forest height			Above-ground biomass		
					MAE (t ha^{-1})	RMSE (t ha^{-1})	R^2	MAE (m)	RMSE (m)
Aragon	2021	2021	3511	0.45	3.2	5.0	0.36	49.5	62.5
Castile la Mancha	2020	2020	5342	0.44	3.1	4.8	0.39	43.6	52.4
Castile and Leon	2019	2019	7428	0.56	3.3	5.0	0.36	44.0	58.4
Catalonia	2017	2016	814	0.16	4.3	6.9	0.15	48.7	59.6
Extremadura	2017	2017	1269	0.53	2.6	3.7	0.35	37.2	46.6
Basque Country	2021*	2022	435	0.45	6.5	8.9	0.16	80.9	97.9

*regional forest inventory data.

Table 6 Comparison of GEDI (rh98) and ALS (P98) heights by region. Positive ME indicates GEDI overestimation.

Region	R^2	RMSE (m)	rRMSE (%)	MAE(m)	ME (m)	N
Andalusia	0.43	3.9	90.1	2.5	2.4	475
Aragon	0.59	6.5	101.5	4.7	4.3	190
Asturias	0.46	9.9	91.6	7.6	6.7	275
Cantabria	0.42	7.9	84.0	5.6	3.4	488
Castile la Mancha	0.31	5.2	129.4	3.2	3.0	157
Castile and Leon	0.48	6.8	101.5	4.6	4.3	45
Extremadura	0.55	3.4	75.6	2.4	2.1	223
Madrid	0.51	4.0	78.4	3.0	1.9	188

high-resolution estimates of forest structural attributes. By integrating data from two lidar surveys conducted over a span of more than a decade, we derived spatially consistent regional maps of forest canopy height, cover, and biomass, and quantified temporal changes at multiple scales. These results have important implications for forest monitoring, disturbance assessment, and carbon accounting as detailed below.

Forest structural changes: growth and heterogeneity

Our results confirm a general increase in forest canopy height and canopy cover between the first and second lidar survey, with average national annual increases of 0.2 m and 0.9%, respectively. These trends are in line with gains reported across southern Europe following afforestation, forest maturation, and rural abandonment (Delgado-Artés *et al.* 2022). However, the observed structural changes are not homogeneous across space. The Atlantic forests exhibited faster structural development, likely driven by more favorable moisture regimes and intensive management of productive species such as *Eucalyptus globulus* and *Pinus radiata*.

In contrast, Mediterranean and semi-arid regions exhibited slower changes likely constrained by limited water availability and greater disturbance exposure (e.g., wildfires, droughts). Such spatial variation reflects the strong influence of regional climatic gradients, forest composition, and management histories on forest dynamics. For instance, the highest AGB values were associated with mesic, late-successional species such as *Fagus sylvatica* and *Quercus robur*, while the lowest biomass was found in drought-adapted, open-canopy species like *Pinus halepensis*.

Species-based analyses reveal that structural metrics vary strongly by dominant taxa and environmental conditions. Atlantic conifers like *P. radiata* and *P. sylvestris* reach heights of up to 16 m and exhibit dense canopies (FCC > 60%), while Mediterranean counterparts remain shorter (typically <12 m) and sparser. Similarly, broadleaf deciduous species like *F. sylvatica* and

Q. robur maintained higher biomass densities than Mediterranean oaks (*Q. ilex, Q. suber*), with AGB values exceeding 180 t ha⁻¹ in mesic zones versus <35 t ha⁻¹ in xeric ones. These findings underline the importance of incorporating species identity in forest monitoring efforts and emphasize the divergent growth trajectories and ecological constraints shaping forest dynamics across bioclimatic regions.

Accuracy of lidar-derived estimates

Validation against NFI *in-situ* measurements confirmed the robustness of the lidar-derived forest metrics. High correlations and relatively low RMSE values for canopy height (e.g., R^2 > 0.8 and RMSE < 3 m in the Basque Country) underscore the potential of PNOA-Lidar surveys for operational forest monitoring.

Accuracy varied substantially across regions and was strongly influenced by the temporal mismatch between field and airborne acquisitions. Temporal gaps exceeding one year generally resulted in degraded error metrics, particularly for canopy cover estimates. This reinforces the importance of synchronizing ground and remote sensing data collection, for calibration and validation purposes, by aligning with *in-situ* monitoring cycles. Further, the accuracy of AGB predictions was moderate (e.g., rRMSE between 40 % and 60% in most regions), and declined in areas with limited plot data or greater structural complexity. Relative errors were higher in Aragon, Galicia, and Extremadura, where forest composition is more heterogeneous or temporal misalignments with NFI data were more pronounced.

These findings underscore the need to account for local variability and sampling intensity when calibrating biomass models, and to adopt correction approaches for temporal inconsistencies, such as the productivity-based adjustment implemented in this study. The relatively large difference between *in-situ* FCC measurements and ALS derived values were expected as NFI uses ocular estimates which are operator and viewing-geometry dependent whereas ALS FCC is a repeatable, physically defined metric derived from the proportion of

laser pulses intercepted by the canopy within a precisely defined footprint (and height threshold).

Benchmarking global products: the value of national ALS data

Our results also provided insights into the performance of regional and global vegetation height products. The comparison between ALS-derived heights and satellite-based datasets revealed large discrepancies, particularly for the structurally complex Atlantic forests. While the Iberian-scale product by Su et al. (2025) showed the highest agreement with ALS data (e.g., MAE < 2.5 m in several regions), global products such as those by Tolan et al. (2024) and Lang et al. (2023) presented substantially higher biases (under- or over-estimations) across all regions.

The independent validation of Su et al. (2025) products, using ALS-derived canopy height (98th percentile), showed large variations in RMSE across biomes. While for the Mediterranean biome the observed RMSE (~2.2–2.7 m) was largely aligned with the stated value (2.19 m), for the Atlantic biome the RMSE doubled (> 4 m), which is likely related to models training in Mediterranean regions (Castile and Leon and Extremadura) and their application to the entire Iberian Peninsula.

Our analysis demonstrates that the Su et al. (2025) height models are biased toward Mediterranean forest structures and fail to generalize in Atlantic regions, as the training data are not representative of the full forest diversity of the Iberian Peninsula.

Similar issues were observed for Su et al. (2025) AGB models which were trained with NFI data from the same two regions.

The independent validation using NFI plots (measured between 2017 and 2021) revealed RMSE values reaching 97.9 Mg/ha in high-biomass regions like the Basque Country, compared to the published RMSE of 40.28 Mg/ha. This discrepancy, particularly pronounced in regions with intensive forestry (e.g., *Pinus radiata* plantations), confirms significant extrapolation errors. For example, the AGB error in the Basque Country is 2.8 times higher than the reported one. In addition, when compared to the regionally trained biomass models developed in this study, the RMSE error of Su et al. (2025) more than doubled in some regions. These findings highlight the limitations of models trained on geographically or structurally unbalanced datasets and emphasize the need for broader and more representative training data when developing products across large areas.

Our comparison with GEDI-derived heights also indicates significant limitations of this spaceborne mission, most likely related to the footprint size, geolocation accuracy, and vegetation terrain complexity, as shown by generally low R^2 and high RMSE values, particularly in mountainous regions like Asturias. The consistent overestimation of canopy height by GEDI (+5.9 m) is primarily attributable to the system's waveform sensitivity to upper canopy elements and its larger footprint size (~25 m), which integrates returns from both tree crowns and terrain variations, particularly in sloped or heterogeneous stands. The observed RMSE are slightly higher when compared to previous studies analyzing the GEDI derived products in Spain (Dorado-Roda *et al.* 2021). This may be related to the much larger extent used in this study and the inclusion of tall forest on complex terrain in the north.

Such comparisons highlight limitations of existing regional and global maps related to reduced sensitivity to local structural variability, particularly in deciduous and mixed forests. In this context, national ALS programs such as PNOA offer a critical benchmark for evaluating satellite-derived products reliability for carbon and ecosystem monitoring frameworks. The harmonized, wall-to-wall lidar database developed in this study can thus serve as a reference for calibration or validation of spaceborne missions derived products.

Limitations

While this study demonstrates the value of harmonized, multi-temporal airborne lidar data for national forest monitoring, several limitations and potential biases need to be acknowledged. The accuracy of aboveground

biomass (AGB) models is inherently influenced by the structural heterogeneity of forest stands and the availability of representative field data.

In regions with complex canopies, such as the mixed Atlantic forests, the relationship between lidar metrics and biomass can become nonlinear due to high vertical layering, understory contributions, and species-specific allometries not fully captured by general models. Likewise, data sparsity, particularly the uneven distribution of National Forest Inventory (NFI) plots across bioclimatic zones, can limit the robustness of machine-learning models in structurally diverse or less-sampled areas. These factors likely contribute to the higher uncertainties observed in Galicia and Extremadura, where forest composition and structure are especially variable.

Temporal differences between NFI field measurements and lidar acquisitions represent another important source of uncertainty. Even after applying productivity-based corrections to harmonize biomass estimates, residual errors may persist when growth or disturbance dynamics differ from regional averages. The analysis showed that the precision of lidar-derived estimates decreased notably when the lag between datasets exceeded one year, particularly in rapidly growing Atlantic forests. This sensitivity underscores the need for closer temporal alignment between ground and remote-sensing surveys and for the adoption of dynamic correction models that account for forest type, age, management and disturbances.

Although the harmonized workflow developed here is transferable, the specific model calibrations and error structures are conditioned by the ecological, climatic, and management contexts of peninsular Spain. The predictive relationships and performance metrics may not directly extrapolate to regions with different forest types, canopy architectures, or disturbance regimes. Nevertheless, the methodological framework is broadly applicable and could support similar large-scale forest monitoring initiatives elsewhere.

Conclusions

This study provides an overview of forest structural dynamics across peninsular Spain using the first two national airborne lidar surveys from the PNOA program. Through standardized processing and machine-learning models calibrated with National Forest Inventory data, we produced the first spatially consistent, wall-to-wall maps of canopy height, canopy cover, and aboveground biomass for the peninsular Spain. These products enable quantification of structural change over more than a decade at high spatial resolution and with lower estimation errors than commonly used satellite-derived rlsrge scale datasets.

Overall, we detected an increase in forest growing stock, with Atlantic forests showing the strongest structural development, while Mediterranean and semi-arid regions exhibited slower gains. These spatial patterns underscore the role of bioclimatic context and forest management in shaping long-term structural dynamics. Our accuracy analysis indicates that lidar-derived height estimates are highly reliable when field and airborne observations are temporally aligned, but precision declines when the time lag exceeds one year, particularly in Atlantic forests. This result supports closer synchronization of national forest inventories and remote-sensing acquisitions in future monitoring campaigns.

Comparisons with satellite-based canopy height and above ground biomass products revealed systematic biases and marked regional variability in performance, reinforcing the importance of airborne lidar as a benchmark for satellite-derived forest structure information. The methodologies and datasets developed here provide a robust foundation for future updates and can support biodiversity assessments, carbon accounting, disturbance mapping, and forest policy implementation. In addition, the derived products can serve as reference data for training satellite-based models to bridge temporal gaps between lidar surveys. Continued investment in coordinated

lidar acquisitions, together with integration of satellite data and ground observations, will be essential to meet emerging forest management challenges.

Conflict of interest

The authors declare no financial or personal interests could influence the work presented in this paper.

Acknowledgements

References

Blanco Castro E., Costa Tenorio M., Morla Juaristi C., Sáinz Ollero H., 2005. Los bosques ibéricos: una interpretación geobotánica. Planeta, Barcelona.

Blondel J. & Aronson J., 1995. Biodiversity and Ecosystem Function in the Mediterranean Basin: Human and Non-Human Determinants. In: Davis G.W. & Richardson D.M. (Eds.), Mediterranean-Type Ecosystems: The Function of Biodiversity. Springer Berlin Heidelberg, Berlin, Heidelberg, pp. 43-119.

Bombín R.V., 2005. El Mapa Forestal de España escala 1:50.000 (MFE50) como base del Tercer Inventario Forestal Nacional. Cuadernos de la Sociedad Española de Ciencias Forestales 19, 205-210.

Bonan G.B., 2016. Forests, Climate, and Public Policy: A 500-Year Interdisciplinary Odyssey. Annual Review of Ecology, Evolution, and Systematics 47, 97-121. https://doi.org/10.1146/annurev-ecolsys-121415-032359.

Breiman, L., 2001. Random Forests. Machine Learning 45, 5-32. https://doi.org/10.1023/A:1010933404324.

Bright B.C., Hudak A.T., McCarley T.R., Spannuth A., Sánchez-López N., Ottmar R.D., Soja A.J., 2022. Multitemporal lidar captures heterogeneity in fuel loads and consumption on the Kaibab Plateau. Fire Ecology 18, 18. https://doi.org/10.1186/s42408-022-00142-7.

Buotte P.C., Law B.E., Ripple W.J., Berner L.T., 2020. Carbon sequestration and biodiversity co-benefits of preserving forests in the western United States. Ecological Applications 30, e02039. https://doi.org/10.1002/eap.2039.

Coops N.C., Tompalski P., Goodbody T.R.H., Queinnec M., Luther J.E., Bolton D.K., White J.C., Wulder M.A., van Lier O.R., Hermosilla T., 2021. Modelling lidar-derived estimates of forest attributes over space and time: A review of approaches and future trends. RSEnv 260, 112477. https://doi.org/10.1016/j.rse.2021.112477

Delgado-Artés R., Garófano-Gómez V., Oliver-Villanueva J.-V., Rojas-Briales E., 2022. Land Use/Cover Change Analysis in the Mediterranean Region: A Regional Case Study of Forest Evolution in Castelló (Spain) Over 50 Years. Land Use Policy 114, 105967. https://doi.org/10.1016/j.landusepol.2021.105967.

Dorado-Roda I., Pascual A., Godinho S., Silva C.A., Botequim B., Rodríguez-González P., González-Ferreiro E., Guerra-Hernández J., 2021. Assessing the Accuracy of GEDI Data for Canopy Height and Aboveground Biomass Estimates in Mediterranean Forests. Remote Sensing, 13(12), 2279; https://doi.org/10.3390/rs13122279.

Dubayah R., Blair J.B., Goetz S., Fatoyinbo L., Hansen M., Healey S., Hofton M., Hurtt G., Kellner J., Luthcke S., Armston J., Tang H., Duncanson L., Hancock S., Jantz P., Marselis S., Patterson P.L., Qi W., Silva C., 2020. The Global Ecosystem Dynamics Investigation: High-resolution laser ranging of the Earth's forests and topography. Science of Remote Sensing 1, 100002. https://doi.org/10.1016/j.srs.2020.100002.

EUROSTAT, 2022. Land cover statistics – Land Use and Cover Area frame Survey (LUCAS). In. European Commission, European Union.

Evans J.S. & Hudak A.T., 2007. A multiscale curvature algorithm for classifying discrete return LiDAR in forested environments. ITGRS 45, 1029-1038.

Fassnacht F.E., Latifi H., Stereńczak K., Modzelewska A., Lefsky M., Waser L.T., Straub C., Ghosh A., 2016. Review of studies on tree species classification from remotely sensed data. RSEnv 186, 64-87. https://doi.org/10.1016/j.rse.2016.08.013.

Freund Y. & Schapire R.E., 1997. A Decision-Theoretic Generalization of On-Line Learning and an Application to Boosting. JCoSS 55, 119-139. https://doi.org/10.1006/jcss.1997.1504.

Friedman J.H., 2001. Greedy function approximation: A gradient boosting machine. The Annals of Statistics 29, 1189-1232. https://doi.org/10.1214/aos/1013203451

Henttonen H.M. & Kangas A., 2015. Optimal plot design in a multipurpose forest inventory. Forest Ecosystems 2, 31. https://doi.org/10.1186/s40663-015-0055-2.

Houghton R.A. & Byers B., Nassikas A.A., 2015. A role for tropical forests in stabilizing atmospheric CO_2. Nature Climate Change 5, 1022-1023. https://doi.org/10.1038/nclimate2869.

Hudak A.T., Fekety P.A., Kane V.R., Kennedy R.E., Filippelli S.K., Falkowski M.J., Tinkham W.T., Smith A.M.S., Crookston N.L., Domke G.M., Corrao M.V., Bright B.C., Churchill D.J., Gould P.J., McGaughey R.J., Kane J.T., Dong J., 2020. A carbon monitoring system for mapping regional, annual aboveground biomass across the northwestern USA. Environ. Res. Let. 15, 095003. https://doi.org/10.1088/1748-9326/ab93f9.

Lang N., Jetz W., Schindler K., Wegner J.D., 2023. A high-resolution canopy height model of the Earth. Nature Ecology & Evolution 7, 1778-1789. https://doi.

org/10.1038/s41559-023-02206-6.

Lines E.R., Zavala M.A., Purves D.W., Coomes D.A., 2012. Predictable changes in aboveground allometry of trees along gradients of temperature, aridity and competition. Global Ecology and Biogeography 21, 1017-1028. https://doi.org/10.1111/j.1466-8238.2011.00746.x.

Matasci G., Hermosilla T., Wulder M.A., White J.C., Coops N.C., Hobart G.W., Zald H.S.J., 2018. Large-area mapping of Canadian boreal forest cover, height, biomass and other structural attributes using Landsat composites and lidar plots. RSEnv 209, 90-106. https://doi.org/10.1016/j.rse.2017.12.020.

Mauro F., Ritchie M., Wing B., Frank B., Monleon V., Temesgen H., Hudak A., 2019. Estimation of Changes of Forest Structural Attributes at Three Different Spatial Aggregation Levels in Northern California using Multitemporal LiDAR. Remote Sensing, 11(8), 923. https://doi.org/10.3390/rs11080923.

McCarley T.R., Kolden C.A., Vaillant N.M., Hudak A.T., Smith A.M.S., Wing B.M., Kellogg B.S., Kreitler J., 2017. Multi-temporal LiDAR and Landsat quantification of fire-induced changes to forest structure. RSEnv 191, 419-432. https://doi.org/10.1016/j.rse.2016.12.022.

Montero G., Ruiz-Peinado R., Muñoz M., 2005. Produccion de biomasas y fijacion de CO_2 por los bosques españoles. Ministerio de Ciencia y Tecnologia, Madrid.

Pan Y., McCullough K., Hollinger D.Y., 2018. Forest biodiversity, relationships to structural and functional attributes, and stability in New England forests. Forest Ecosystems 5, 14. https://doi.org/10.1186/s40663-018-0132-4.

Potapov P., Li X., Hernandez-Serna A., Tyukavina A., Hansen M.C., Kommareddy A., Pickens A., Turubanova S., Tang H., Silva C.E., Armston J., Dubayah R., Blair J.B., Hofton M., 2021. Mapping global forest canopy height through integration of GEDI and Landsat data. RSEnv 253, 112165. https://doi.org/10.1016/j.rse.2020.112165.

Ruiz-Benito P., Gómez-Aparicio L., Paquette A., Messier C., Kattge J., Zavala M.A., 2014. Diversity increases carbon storage and tree productivity in Spanish forests. Global Ecology and Biogeography 23, 311-322. https://doi.org/10.1111/geb.12126 .

San-Miguel-Ayanz J., Durrant T., Boca R., Maianti P., Liberta G., Oom D., Branco A., De Rigo D., Ferrari D., Roglia E. and Scionti N., 2023. Advance Report on Forest Fires in Europe, Middle East and North Africa 2022. In, Luxembourg. https://doi.org/10.2760/091540.

Sanz V. & Soto V.D., 1990. Segundo Inventario Forestal Nacional 1986-1995 Explicaciones y metodos. EGRAF S.A., Madrid.

Senf C. & Seidl R., 2020. Mapping the forest disturbance regimes of Europe. Nature Sustainability 4, 63-70.

https://doi.org/10.1038/s41893-020-00609-y.

Senf C., Seidl R., Hostert P., 2017. Remote sensing of forest insect disturbances: current state and future directions. IJAEO, 60, 49-60. https://doi.org/10.1016/j.jag.2017.04.004.

Su Y., Schwartz M., Fayad I., García M., Zavala M.A., Tijerín-Triviño J., Astigarraga J., Cruz-Alonso V., Liu S., Zhang X., Chen S., Ritter F., Besic N., d'Aspremont A., Ciais P., 2025. Canopy height and biomass distribution across the forests of Iberian Peninsula. Scientific Data 12, 678. https://doi.org/10.1038/s41597-025-05021-9.

Tanase M., Martini J.P., Miranda P., Garcia D., Wilke V., Miguel S., Mihai C., Diez J., Natal S., Martin D.S., Astigarraga J., Ruiz-Benito P., 2026. Long-term forest structure trends in the peninsular Spain from lidar-optical sensors synergies. RSEnv 334. https://doi.org/10.1016/j.rse.2025.115196.

Tolan J., Yang H.-I., Nosarzewski B., Couairon G., Vo H.V., Brandt J., Spore J., Majumdar S., Haziza D., Vamaraju J., Moutakanni T., Bojanowski P., Johns T., White B., Tiecke T., Couprie C., 2024. Very high resolution canopy height maps from RGB imagery using self-supervised vision transformer and convolutional decoder trained on aerial lidar. RSEnv 300, 113888. https://doi.org/10.1016/j.rse.2023.113888.

Tomppo E., Schadauer K., McRoberts R.E., Gschwantner T., Gabler K., Ståhl G., 2010. Introduction. In: Tomppo, T.G., Lawrence M., McRoberts R. E. (Ed.), National Forest Inventories: Pathways for Common Reporting. Springer, New York, p. 614.

van Ewijk K.Y., Treitz P.M., Scott N.A., 2011. Characterizing Forest Succession in Central Ontario using Lidar-derived Indices. Photogrammetric Engineering & Remote Sensing 77, 261-269. https://doi.org/10.14358/PERS.77.3.261.

van Rees E., 2013. Rapidlasso: Efficient Tools for LiDAR Processing. GeoInformatics 16, 14-16.

Villaescusa R. & Díaz R., 1998. Segundo Inventario Forestal Nacional (1986-1996). In. Ministerio de Medio Ambiente, ICONA, Madrid, p. 337.

White J.C., Coops N.C., Wulder M.A., Vastaranta M., Hilker T., Tompalski P., 2016. Remote Sensing Technologies for Enhancing Forest Inventories: A Review. Canadian Journal of Remote Sensing 42, 619-641. https://doi.org/10.1080/07038992.2016.1207484.

Wulder M.A., Hermosilla T., Stinson G., Gougeon F.A., White J.C., Hill D.A., Smiley B.P., 2020. Satellite-based time series land cover and change information to map forest area consistent with national and international reporting requirements. Forestry: An International Journal of Forest Research 93, 331-343. https://doi.org/10.1093/forestry/cpaa006.